

Paper IBC 17-89

34<sup>th</sup> International Bridge Conference

Gaylord National Resort, National Harbor, MD

June 5-8, 2017

**Title: Low-Cost Scour Preventing  
Fairings for Bridges**

ROGER L. SIMPSON, Ph.D., P.E., M.ASCE corresponding author

Email: [rogersimpson@aurinc.com](mailto:rogersimpson@aurinc.com)

Phone: (540)-961-3005

FAX: 866-223-8673

GWIBO BYUN, Ph.D.

Email: [Gwibo@aurinc.com](mailto:Gwibo@aurinc.com)

Phone: (540)-553-5139

FAX: 866-223-8673

Applied University Research, Inc.

605 Preston Avenue

Blacksburg, VA 24060-4618

KEYWORDS: Bridge scour prevention; scour-vortex prevention;

bridge piers; abutments; vortex generators

## **Abstract**

Cost-effective optimized robust scour preventing three-dimensional convex-concave hydrodynamic fairings (sCAUR™) with attached counter-scour vortex generators (VorGAUR™) have been designed, developed, extensively tested at model and full scale under NCHRP-IDEA sponsorship, and are now available for practical use for bridge piers and abutments. Their particular shape prevents creation of scouring vortices that cause the local scour problem for any river level, speed, and angles of attack up to 20 degrees (45 degrees with a "dog-leg). Many advantages are discussed.

## **Introduction- Background of Bridge Pier and Abutment Scour**

Removal of river bed substrate around bridge pier and abutment footings, also known as scour, presents a significant cost and risk in the maintenance of many bridges throughout the world and is one of the most common causes of highway bridge failures (1). In a recent work (2), it is estimated that over 70% of US bridges were not designed for scour prevention and that peak flows during floods cause most scour and failures over a short period of time. It has been estimated that 60% of all bridge failures result from scour and other hydraulic-related causes (3). This has motivated research on the causes of scour at bridge piers and abutments (4) and led bridge engineers to develop numerous countermeasures that attempt to reduce the risk of catastrophe. Unfortunately, all previously used countermeasures are temporary responses that require many recurring costs and do not prevent the formation of scouring vortices, which is the root cause of the local scour (5,6). Consequently, sediment such as sand and rocks around the foundations of bridge abutments and piers is loosened and

carried away by the flow during floods, which may compromise the integrity of the structure. Even designing bridge piers or abutments with the expectation of some scour is highly uncertain, since a recently released study (5) showed huge uncertainties in scour data from hundreds of experiments. None of the conservative current bridge pier and abutment footing or foundation designs prevent scouring vortices, which are created when the flow interacts with underwater structures, so the probability of scour during high water or floods is present in all previous designs.

The bridge foundations in a water current, such as piers and abutments, change the local hydraulics drastically because of the appearance of large-scale unsteadiness and shedding of coherent vortices, such as horseshoe vortices. Figure 1a is a sketch of the horseshoe vortex formed around the base of a pier by a separating boundary layer. The horseshoe vortex produces high bed shear stress, triggers the onset of sediment scour, and forms a scour hole. (See [www.noscour.com](http://www.noscour.com).)

The flowfield around an abutment is also highly three-dimensional and involves strong separated vortex flow (7). For a vertical abutment shown in Figure 1b, a separation bubble is formed at the upstream corner of the abutment. Unsteady shed wake vortices are created due to the separation of the flow at the abutment corners. These wake vortices are very unsteady, are oriented approximately parallel to the abutment edge and have low pressure at the vortex cores. These vortices act like small tornadoes, lifting up sediment and creating a large scour hole behind the abutment. The downflow at the front of the abutment is produced by the large stagnation pressure gradient of the

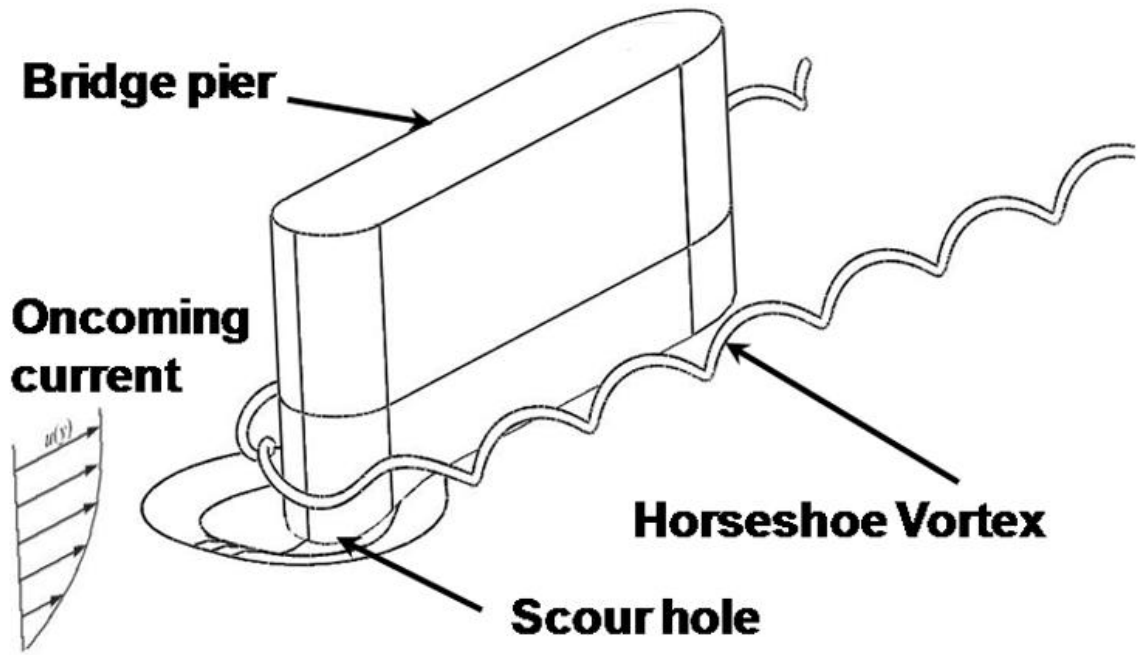


Figure 1a. The formation of a horseshoe vortex around the bottom of a bridge pier with no scouring-vortex prevention.

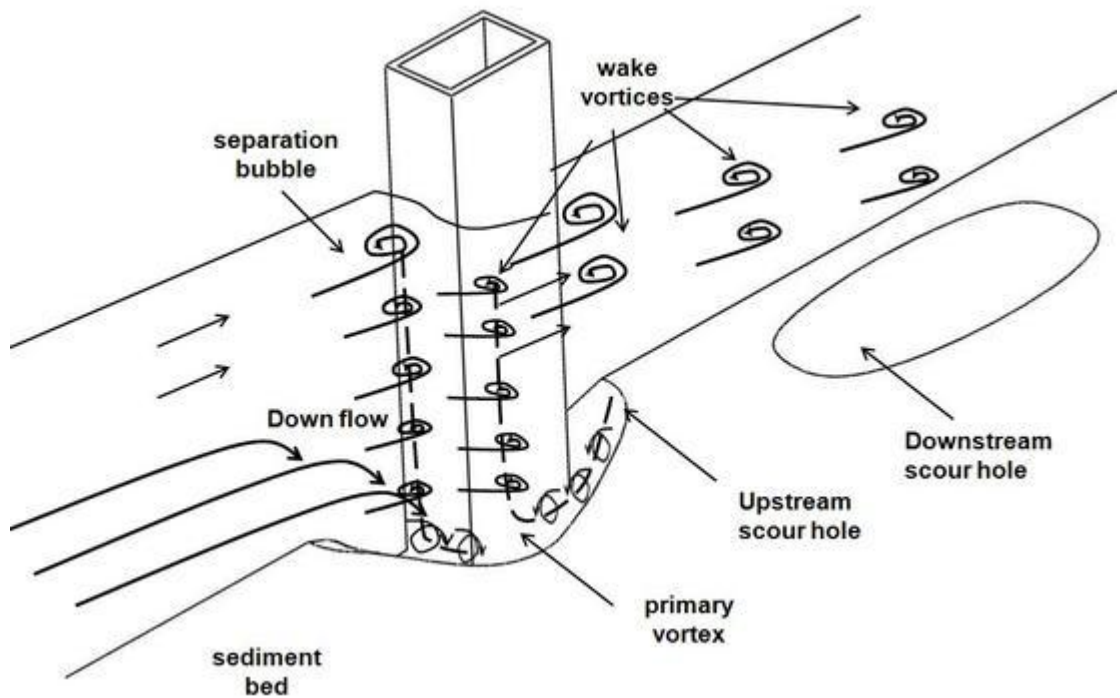
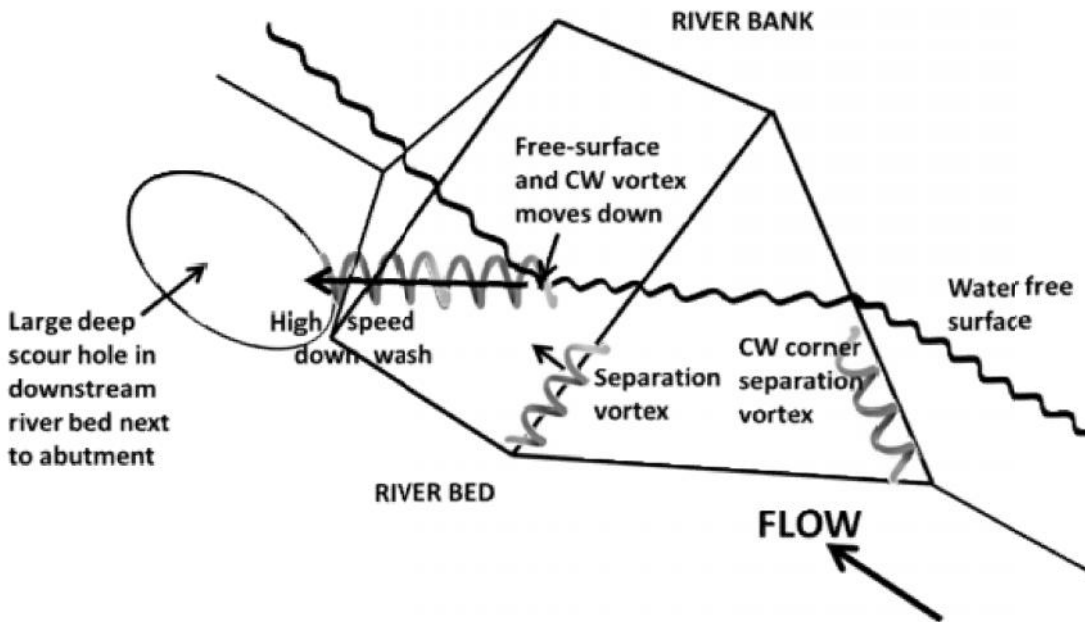


Figure 1b. . The formation of a scouring vortices around a vertical abutment with no scouring-vortex prevention. approaching flow. The down flow rolls up and forms the primary

vortex, which is similar to the formation of the horseshoe vortex around a single bridge pier.

**Spill-through abutment**  
**without scour countermeasures**



**Figure 1c. Flow structure around the spill-through abutment with no scouring vortex protection.**

For the spill-through abutment with no scour protection, the flow is accelerated around the contraction and separated downstream of the contraction leading edge as shown in Figure 1c. There is a free surface level difference before and after the contraction leading edge due to the free surface vortex formation. The spill-through abutment has the scour hole at the downstream of the model with the similar order of depth of the vertical square corner wall due to the free surface vortex generated at the leading edge of the contraction.

It should be noted that rip rap countermeasures are not acceptable design elements for new bridges (1). To avoid liability risk to engineers and bridge owners, new bridges must

be over-designed to withstand 500-year superfloods, assuming that all sediment is removed from the 'scour prism' at that flow rate (1). Unlike temporary scour countermeasures, the streamlined control Against Underwater Rampage fairing sCAUR™ (pronounced like 'scour') designs avoid liability risk by preventing or drastically diminishing the scour prism and reducing the cost of new bridge engineering and construction. This greatly reduces the probability of failure, by the tenets of catastrophic risk theory (8). See [www.noscour.com](http://www.noscour.com) for more details.

### **Features of sCAUR™ that Prevent Scouring Vortices**

Using the knowledge of how to prevent the formation of discrete vortices and separation for junction flows (9,10,11), prior to the NCHRP-IDEA-162 project, AUR developed, proved using model-scale tests, and patented new local-scouring-vortex-prevention sCAUR™ products. The sCAUR™ design fundamentally alters the way the river flows around a pier or abutment. The sCAUR™ scouring-vortex preventing fairing, US Patent No. 8,348,553, and VorGAUR™ tetrahedral vortex generators, US Patent No. 8,434,723, are practical long-term permanent solutions. Piecewise continuous slope and curvature surface versions from sheet metal have been proven to produce the same result (US Patent no. 9,453,319, Sept. 27, 2016). A hydraulically optimum pier or abutment fairing prevents the formation of highly coherent vortices around the bridge pier or abutment and reduces 3D separation downstream of the bridge pier or abutment with the help of the VorGAUR™ vortical flow separation control (Figure 2). This is in contrast to a fairing shape used in an unpublished FHWA study which did not prevent scour for flows at angles of attack.

Recent NCHRP research using hundreds of sets of scour data (5) shows that model-scale bridge scour experiments produce much more severe scour depth to pier size ratios than the scour depth to pier size ratios observed for full-scale cases due to scale or size effects. Thus, the scAUR™ fairing will work just as well in preventing the scouring vortices and any scour at full scale as at the proven model scale.

### **Recent NCHRP-IDEA-162 Project**

This project focused on providing more evidence that the scAUR™ and VorGAUR™ concepts and products work at full scale in preventing scour-producing vortices and for a wider range of geometries and conditions. Task I, which is not discussed further here, dealt with selecting a scour-critical bridge in Virginia for prototype installation (8). Further computational work on the effect of pier size or scale (Task II) and model flume tests for other sediments (Task III), other abutment designs (Task IV.A), and for open bed scour conditions (Task IV.B) were done to expand confidence in these concepts and designs. Constructed full-scale prototypes (Task V, not discussed here) were tested (Task VI). Cost-effective manufacturing and installation of scAUR™ and VorGAUR™ products were further developed (Task VII).

### **TASK II - Computational Fluid Dynamic (CFD) Calculations for a Full-scale Pier compared to low Reynolds Number Model-scale CFD**

While much previous AUR computational and experimental work at model size ( $Re_t = 1.34 \times 10^5$ , pier width  $t = 0.076\text{m}$ ) was done to prove these designs, Reynolds number and bridge pier size effects were examined using computations to confirm the applicability of these products at full scale ( $Re_t = 2.19 \times 10^6$ ,  $t$

= 0.624m). Since the V2F Reynolds-averaged Navier-Stokes (RANS) model in the Open Foam code is proven to accurately compute 3D flows and the presence of any separation or discrete vortices (8,9,10,11,12,13), then the behavior of mean streamlines, the local non-dimensional surface pressure coefficient  $C_p$ , and the local surface skin friction coefficient  $C_f$  are sufficient to determine if any separation or discrete vortices are present(8).

Low Reynolds Number Case - Near wall streamlines pass through  $X/t = 7.24$  and  $Y/t = 0.013$

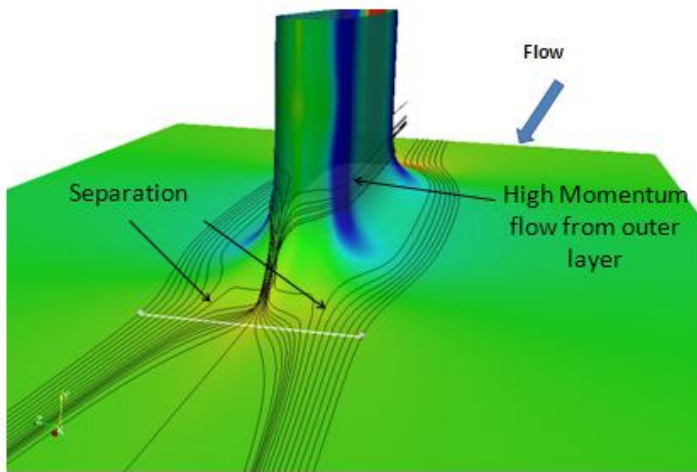


**Figure 2 Low Reynolds number case CFD calculated flow streamline patterns around a sCAUR™ streamlined bridge pier fairing. Flow indicates no discrete vortex formation on nose and sides.**

Figure 2 shows a perspective view from downstream of near-wall streamlines that pass through  $X/t = 7.24$  at  $Y/t = 0.013$ , where  $t$  is the pier width. No vortices or separation are observed upstream of the stern or tail of the pier and there are similar streamline features for both Reynolds numbers. An important feature in the  $C_p$  and the  $C_f$  results is the lack of any abrupt changes in the slope of  $C_p$  or  $C_f$  over a short distance, which means that there is no discrete vortex formation and separation. The non-dimensional drag on the pier is clearly lower for the

higher Reynolds number case because  $C_f$  is always lower and the overall drag is an integral of the surface shearing stress over the pier surface area. In addition, these results show lower flow blockage than without the scAUR™ and VorGAUR™ products because low velocity swirling high flow blockage vortices are absent. As a result, water moves around a pier or abutment faster near the river surface, producing a lower water level at the bridge and lower over-topping frequencies on bridges during flood conditions for any water level when no discrete vortices are present.

Based on the past published work on scour and the experience of AUR (9, 10, 11), more physical evidence and insights support the idea that these scour vortex preventing devices will work better at full scale than model scale. Scouring forces on river bed materials are produced by pressure gradients and turbulent shearing stresses, which are instantaneously unsteady. At higher Reynolds numbers and sizes, pressure gradients and turbulent fluctuation stresses are lower than at model scale, so scour at the same flow speed is lower. **Work by others (4,5,14) supports the conclusion that scour predictive equations, developed largely from laboratory data, overpredict scour on full-scale underwater structures. Thus, the scAUR™ and VorGAUR™ work as well or better in preventing the scouring vortices and any scour at full scale as at the proven model scale.** Other CFD by AUR, which is discussed below, shows that scAUR™ and VorGAUR™ products also prevent scouring vortices around bridge piers downstream of bending rivers.

### **TASK III Flume Tests with Several Smaller Size Sediments at Model Scale**

Data on the performance of the scAUR™ fairing and VorGAUR™ VGs were obtained using several smaller size sediments at model scale in the AUR flume to prove the applicability of the designs for fine sediments (8). All tests were at a flow speed of 0.66mps when incipient open bed scour of the pea gravel (3.2mm to 6.3mm) was first observed. Melville (15) states that the greatest equilibrium scour depth occurs around a circular pier (width = t) when it is surrounded by uniform sediment at times when the flow velocity equals the critical value, i.e., incipient conditions for open bed scour. Also, live bed scour depth is never larger than incipient scour depth. Melville states: "Recent data by Sheppard et al. (14) demonstrate significant scour depth reductions for increasing t/d50 when t/d50 > 50. Thus, local scour depths at field scale may be significantly reduced from those observed in the laboratory." The "t/d50" term is the ratio of pier width to median grain diameter. A value of t/d50=50 was used, with a range of sediments from 38.1 to 64.6.

Three sieved sand or gravel sizes were used to encompass this range for previously reported flow conditions where scour will be the greatest for the AUR t = 76.2mm wide model pier: Gravel A: 1.18 to 1.4 mm; Gravel B: 1.4 to 1.7mm; Gravel C: 1.7 to 2mm. Usually smaller sediment scours before larger pea gravel. No scour around the scAUR™ model occurred for any of these black slag gravel at speeds when the open bed pea gravel began to scour (8) within the  $y/t = +/- 0.004$  measurement uncertainty.

#### Task IV.A - Flume Tests of SCAUR™ and VorGAUR™ Concepts for a Larger Class of Abutments

The performance of scAUR™ and VorGAUR™ concepts for wing-wall

and spill-through abutments was examined by model scale flume tests at incipient open bed scour flow speeds of 0.66mps (8) and show that sCAUR™ and VorGAUR™ prevent the formation of scouring vortices and scour.

Figure 3 shows surface oilflow results for a sCAUR™ modified wing-wall abutment with VorGAUR™ vortex generators (VGs)(8). The mixture of yellow artist oil paint and mineral oil flows with the skin friction lines. Yellow streaks are first painted about perpendicular to the flow direction on a black painted surface. The flow causes some oil to be carried downstream in a local flow direction, which can be observed against the black painted surface. **Figure 3 clearly shows that the effects of the sCAUR™ with VorGAUR™ are to bring lower velocity flow up from the flume bottom and prevent the scour around the bottom of the abutment.**

**With a sCAUR™ modified wing-wall abutment with VGs, there is not only no scour around the model base (Figure 4), but there is no open bed scour hole farther downstream of the model around  $x/L = 2$ .** This is because the VGs generate counter-rotating vortices which diffuse and reduce the strength of the free-surface generated vortex, which caused the scour hole farther downstream of the model for the untreated case.

Flow and scour depth results are given for flume tests without and with sCAUR™ modified spill-through abutment with VorGAUR™ VGs under the same 0.66mps flow (8). The surface oilflow (Figure 5) clearly shows that the sCAUR™ and VorGAUR™ products bring lower velocity flow up from the flume bottom and prevent scour around the bottom of the abutment. Deep scour holes occur around the foundation for the untreated spill-through abutment (8).

Figure 6 shows no scour around the upstream contraction and near the base of the modified spill-through abutment due to the fairing. Although there is still a very minor scour at the downstream of the model, its max depth ( $-0.02L$ ) is much lower than that for an untreated abutment. **The open bed scour due to the free surface vortex has been prevented.**

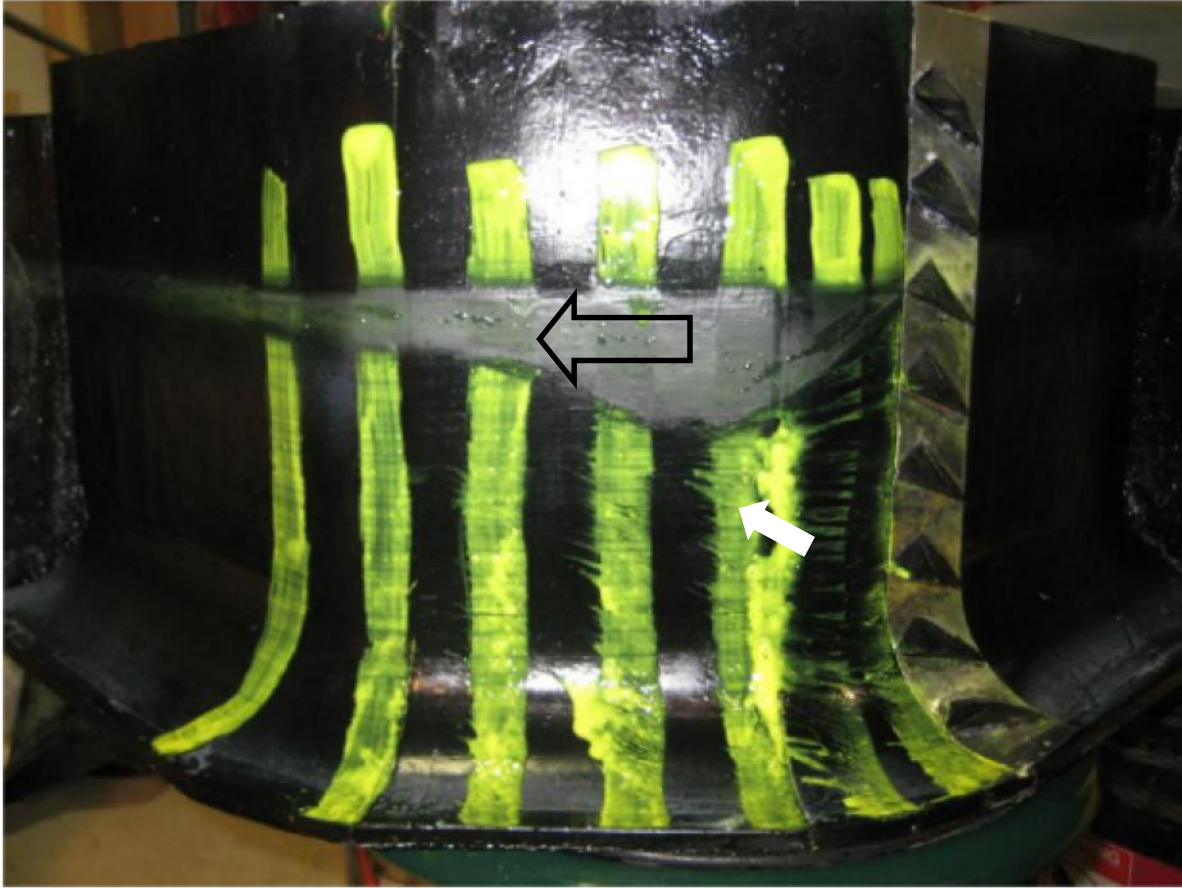


Figure 3. Surface oilflow results for the modified wing-wall abutment model with VGs. Flow from right to left. The upward streaks show that sCAUR™ and VorGAUR™ products cause the flow to move up the abutment. The gray region is produced by a mixture of the oilflow material and waterborne substances at the free surface.

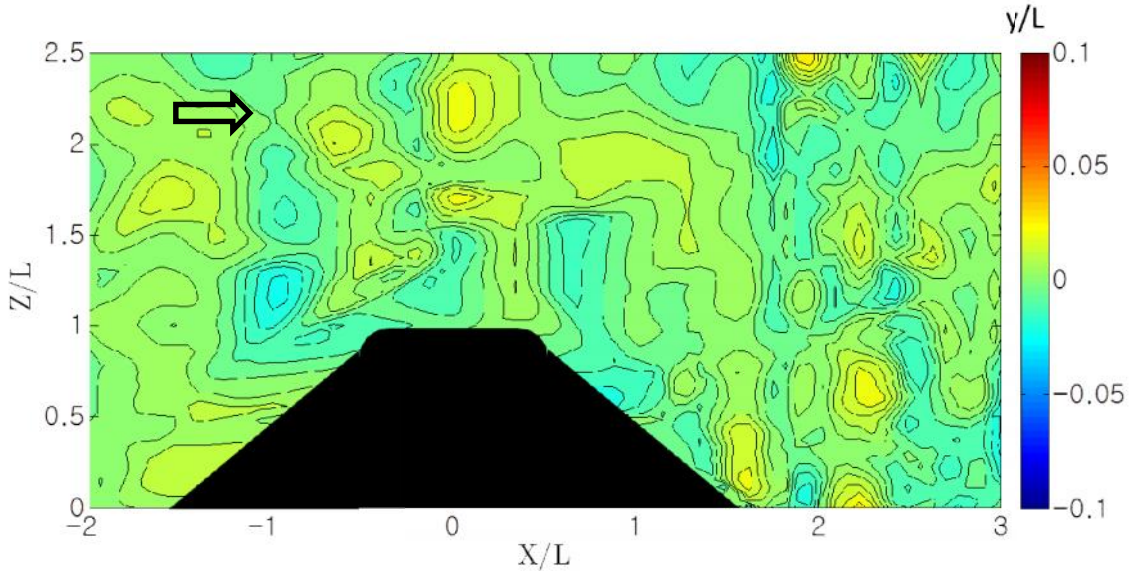


Figure 4. Contours of bed level change after and before flow around the sCAUR™ modified wing-wall model with VorGAUR™ VGs.  $L$  is the abutment length into the flow. No scour at any location (8).

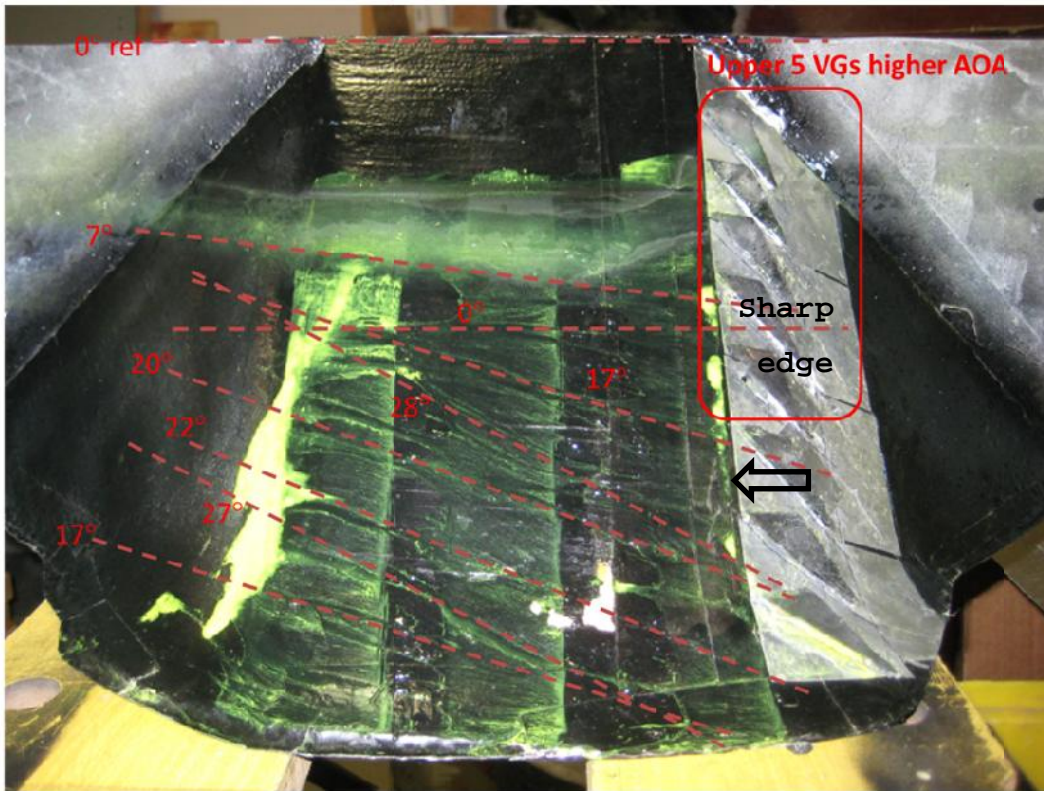


Figure 5. Surface oilflow results for modified sharp-edge spill-

through abutment model with 8 VGs. Note that sCAUR™ and VorGAUR™ cause the flow to move up the abutment as it moves downstream, bringing low speed fluid from the bottom of the river and preventing scour. The gray region is produced by a mixture of the oilflow material and waterborne substances at the free surface (8).

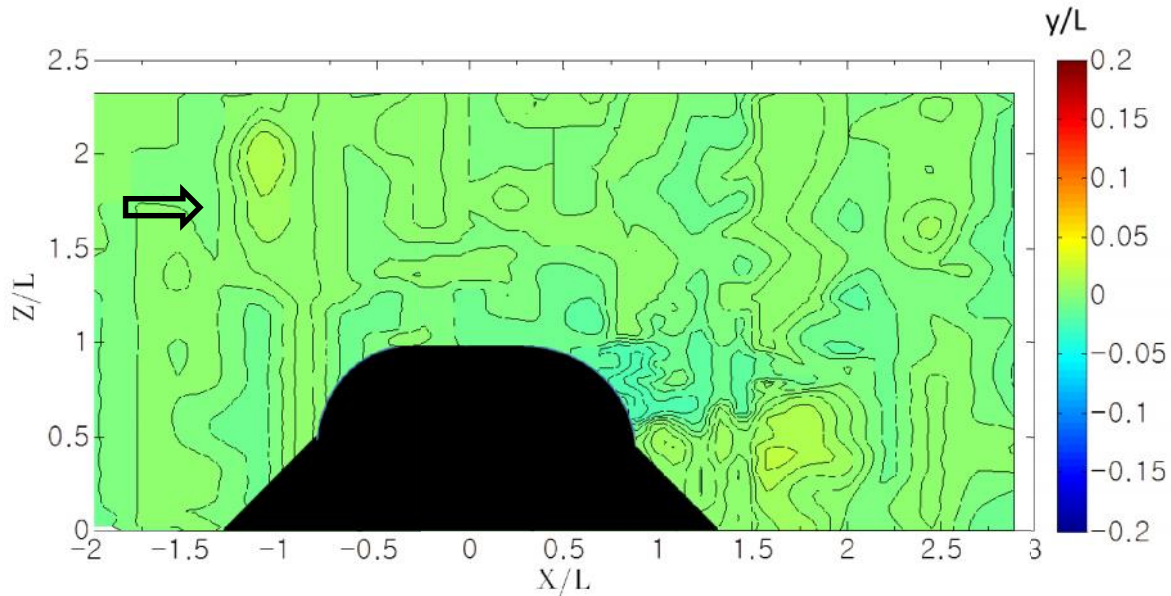


Figure 6. Contours of bed level change after and before flow around the sCAUR™ modified sharp-edge spill-through model with VorGAUR™ VGs (L = 229mm). No scour at any location (8).

#### TASK IV.B - Flume Tests of Foundations Exposed by Open Bed Scour

Aspects of the sCAUR™ and VorGAUR™ design features have been expanded for use around the foundation (US Patent 9,453,319, Sept. 27, 2016) to protect the foundation from the effects of contraction scour, long term degradation scour, settlement and differential settlement of footers, undermining of the concrete sCAUR™ segments, and effects of variable surrounding bed levels. As all AUR flume studies have shown (8), under these conditions scour of the open bed material occurs at a lower river speed before scour of the material around the base of the sCAUR™

fairing occurs.

This means that scour of the river bed away from the sCAUR™ protected pier or abutment occurs first and that the river bed level will be lower away from the pier or abutment. If a pier or abutment foundation is exposed, it will still have a higher immediate surrounding river bed level than farther away. Even so, one would like to further arrest scour around the foundation to prevent high speed open bed scour from encroaching on the river bed material next to the foundation.

Second, if the front of the foundation of a pier or abutment is exposed to approach flows, then a foundation horseshoe or scouring vortex is formed at the front which will cause local scour around the pier or abutment. This suggests that a curved-top ramp be mounted in front of the foundation that prevents the formation of this foundation horseshoe vortex.

Based on these facts, flume tests were conducted with 3 foundation leading edge ramp configurations: (1) an exposed rectangular foundation with no front ramp protection, (2) an upstream curved-top foundation ramp with trapezoidal span-wise edges to produce a stream-wise vortex to bring open bed materials toward the foundation, and (3) a curved-top upstream foundation ramp with straight span-wise edges. Gravel A was used around the foundation since it was the smallest gravel tested in this project in Task III. **In summary, all of these foundation tests show that a leading edge straight-sided curved top ramp prevents scour around a foundation when there is open bed scour, as shown in Figure 7.**



Figure 7. Gravel level after flume test for 12.7mm high elevation with a 12.7mm high straight-sided curved leading edge ramp. No scour is observed (8).

**TASK VI. Tests of Full-Scale sCAUR™ and VorGAUR™ Prototype in the University Of Iowa Institute of Hydraulic Research (IIHR) Flume.**

Full-scale pier model scour tests were conducted during 2013 in the high flow quality University of Iowa Institute of Hydraulic Research (IIHR) 3.05m wide Environmental Flow Facility, which is described at the website:

<http://www.iihr.uiowa.edu/research/instrumentation-and-technology/environmental-flow-facility/>.

Two test gravel sediment sizes (specific gravity = 3) were used during each test. With only a trace amount below 3.2mm, by weight about 63% of the smaller sediment gravel was between 3.2mm and 6.3mm and 37% was between 6.3mm and 9.5mm. The larger test gravel, which filled most of the flume bed, was between 9.5mm and 16mm. A 88.9mm outside diameter vertical circular cylinder model was located downstream of the sCAUR™ model about 0.46m from a flume side wall and 0.46m from the end of the gravel bed and tested with the larger gravel at the same time as each of the several configurations of the sCAUR™ full-scale

model to show that the flow conditions cause scour with the cylinder. Test runs continued until after the cylinder scour reached equilibrium conditions with no further observed scour. With the larger gravel, the equilibrium scour hole was 76mm deep in front of the cylinder and extended 89mm upstream with a span-wise width of 0.28m.

Measurements were obtained for the scour depth around the base of the model after the flume was drained using photos of laser sheet surface locations (6), surface oilflows over the model to determine the local surface flow direction, and some pitot tube flow velocity data in front of and around the model. Five full-scale model configurations were tested with the larger and smaller gravel on opposite sides of the model (8): Configuration A, a full-scale 10.16m long 1.42m wide sCAUR™ model with 6 VorGAUR™ vortex generators with three 2.44m side sections on each side, as shown in Figure 8, flush with the gravel bed top; Configuration B, same as Configuration A, but with 8 VorGAUR™ vortex generators; Configuration C, same as B, but with the straight-sided leading edge curved-top ramp like in Figure 7 above and the model 76mm above the surrounding gravel bed; Configuration D, full-scale sCAUR™ with 8 VorGAUR™ vortex generators with only one side section on each side and flush with the gravel bed; Configuration E, full-scale sCAUR™ nose and tail sections with 4 nose section VorGAUR™ vortex generators with no side sections.

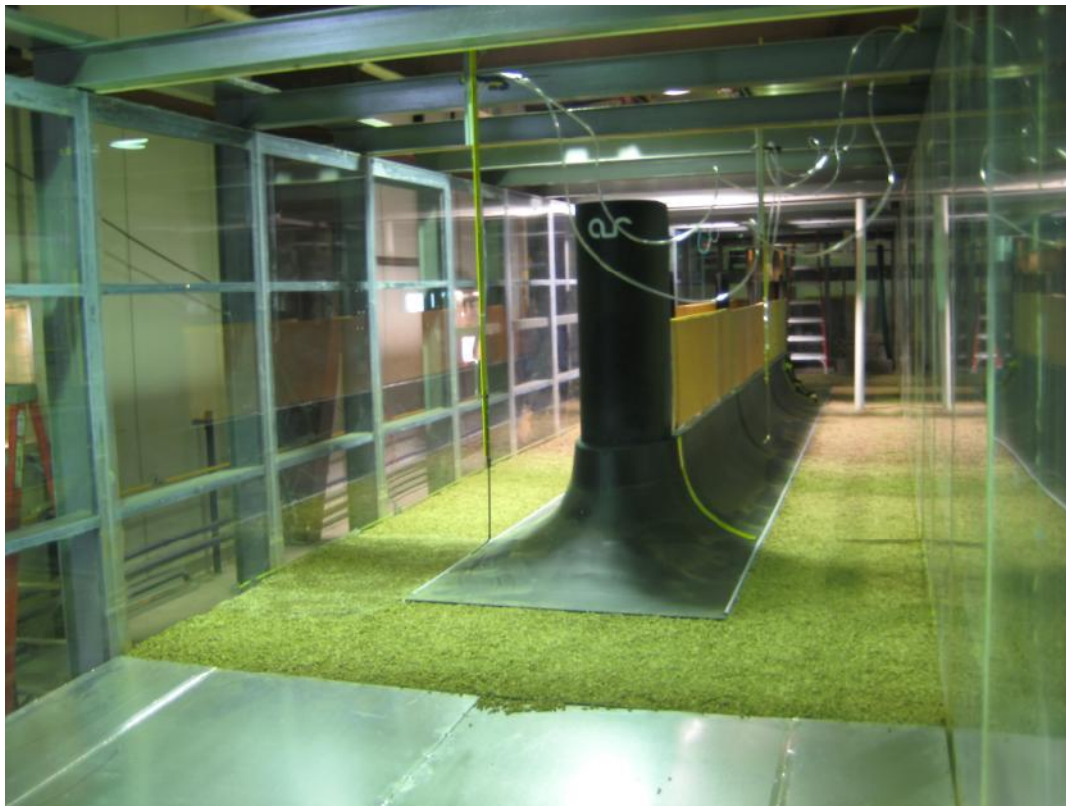


Figure 8. Photo from upstream of the AUR full-scale 10.16m long 1.42m wide sCAUR™ with VorGAUR™ vortex generators model in the IIHR Environmental Flume Facility with three 2.44m side sections on each side for Configurations A and B. Small and large gravel on opposite sides are flush with the edge of the model.

In summary, the full-scale model tests confirmed that there was no scour around the front and sides for each Configuration with either the smaller or larger gravel, as was also observed at model scale. Only a small amount of scour of the smaller gravel was observed downstream, which was due to full-scale model width to flume width (0.15 to 1/3) flow blockage effects, which were comparable to flow blockage results for the 1/7 size models in the AUR flume (8).

#### **TASK VII. Cost-effective Manufacturing and Installation of**

## **sCAUR™ and VorGAUR™ Products**

Before this project, AUR performed a cost-benefit analysis of sCAUR™ with VorGAUR™ as compared to current scour countermeasures (8). Published information shows that current expenses are required for scour monitoring, evaluation, and anti-scour mitigation design and construction, usually with rip-rap. For a bridge closed due to scour, the cost to motorists due to traffic detours is estimated to be as great as all other costs combined, but were not included in the analysis (8).

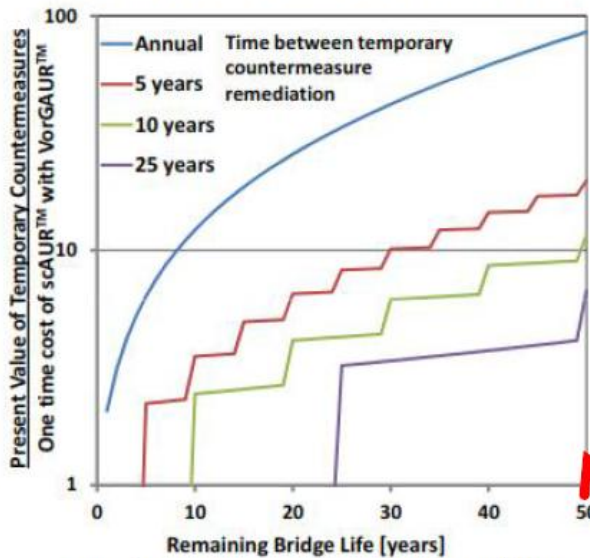
There is no situation where sCAUR™ and VorGAUR™ products cost more than current countermeasures. As shown in Figure 9 for stainless steel retrofits. There is no situation where any type of scour is worse with the use of the sCAUR™ and VorGAUR™ products than without them. The more frequent that scouring floods occur, the more cost effective are sCAUR™ and VorGAUR™. Clearly, sCAUR™ and VorGAUR™ products are practical and cost-effective for US highway bridges (8).

In order to further reduce costs and increase the versatility of the sCAUR™ and VorGAUR™ products, multiple manufacturing alternatives were considered. The required labor, materials, time, logistics, and practical issues were examined and used to evaluate manufacturing alternatives (8). Since the NCHRP-IDEA-162 project, detailed full-scale cost-effective versions have been developed for installation.

### **Retrofit to an Existing Bridge**

An installed welded stainless steel (SS) sCAUR™ retrofit bridge fairing is cost-effective, being about half of all costs for

# Economics of Stainless Steel *scAUR*<sup>TM</sup> Retrofits



Costs of temporary countermeasures obtained from a number of published sources. Computed with 7% inflation and 5% tax exempt interest. **Example of a bridge with six piers and two abutments requiring protection.**

*scAUR*<sup>TM</sup> Manufacturer AUR, Inc.  
[aur@aurinc.com](mailto:aur@aurinc.com)  
 Ph: 540-961-3005 Fax: 866.223.8673.

- Temporary scour countermeasures (TSC) carry compounding future costs (monitoring, inspections, engineering, remediation) with **real present value**.
- *scAUR*<sup>TM</sup> is a permanent sustainable scour prevention measure with a **one-time cost**. **Stainless steel costs ½ as much as concrete.**
- ***scAUR*<sup>TM</sup> prevents catastrophic failure risk and liability due to local scour and saves >90% of present value of TSC.**
- The methods of **HYRISK** used to compare *scAUR*<sup>TM</sup> to temporary countermeasures.
  - Risks from temporary countermeasures incur substantial costs and liabilities.
  - Failure probabilities yield the costs that are implicitly assumed by the bridge owner due to risk.

***scAUR*<sup>TM</sup> is the clear economic choice for bridges with or likely to have severe local scour.**

**Figure 9. Economics of stainless steel retrofits.**

precast or cast-in-place concrete manufacturing and installation (8). Its corrosion resistance gives it a lifetime of 100 years even in seawater environments, using a proper thickness, construction methods, and type of SS. It is an effective way to reduce weight and the cost associated with casting custom reinforced concrete structures. Another benefit is that the SS VorGAUR<sup>TM</sup> vortex generators can be welded directly onto the side sections instead of having to be integrated into the rebar cage of the reinforced concrete structure. Figure 10 is an example of a retrofitted wing-wall abutment. **Even for bridges with little life left, current temporary countermeasures are much more expensive when the present value of future expenses is considered (8).**

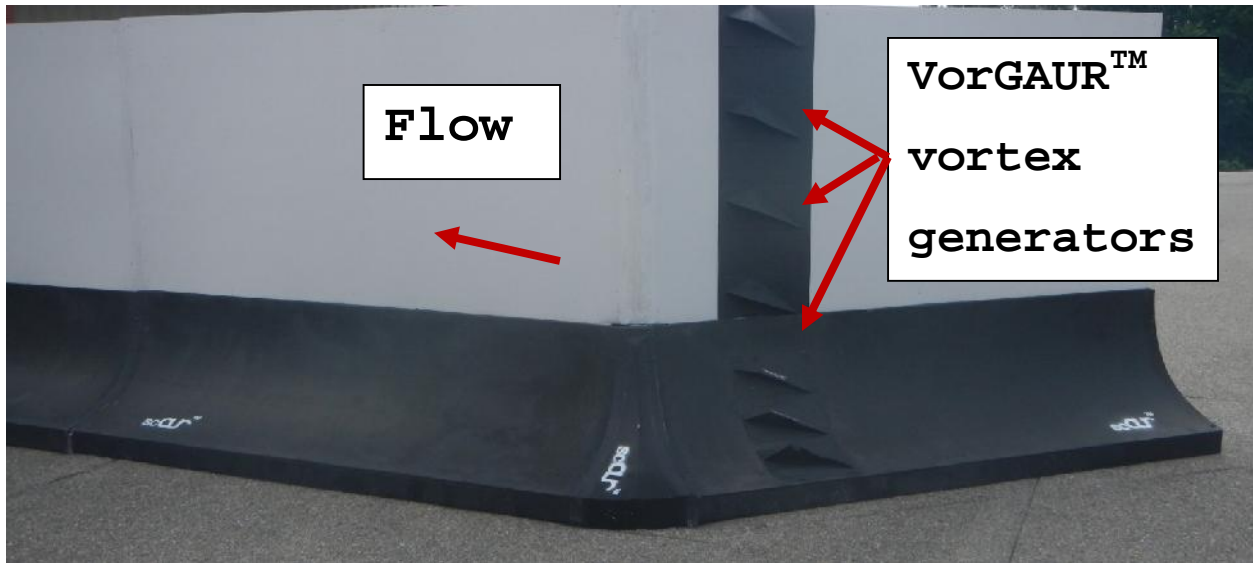


Figure 10. Photo of an example stainless steel sCAUR™ retrofit (black) for a 45° wing-wall abutment. Note stainless steel VorGAUR™ vortex generators.

### New construction

In the case with new construction, essentially the difference between the way cast-in-place bridge piers and abutments are constructed currently without the sCAUR™ products and in the future with the sCAUR™ products is that sCAUR™ steel forms for the concrete are used (8). All standard currently used concrete construction methods and tools can be used. During the bridge design phases, the bridge pier or abutment foundation or footer top surface width and length would need to be large enough to accommodate the location of the sCAUR™ concrete fairing on top. Rebar needed for the sCAUR™ would be included in the foundation during its construction. Stainless steel rebar for welding to the stainless steel vortex generators mounting plates on the surface needs to be used for specific locations. Figure 11 shows example sCAUR™ new construction concrete forms for a pier while Figure 12 shows example sCAUR™ new construction concrete forms for a 45° spill-through abutment. **Clearly, since the new**

construction cost is about 1/3 of retrofit costs, the best time to include the sCAUR™ fairing on piers and abutments is during new construction (8).



Figure 11. Photo of example sCAUR™ new construction concrete forms (black) for a pier.

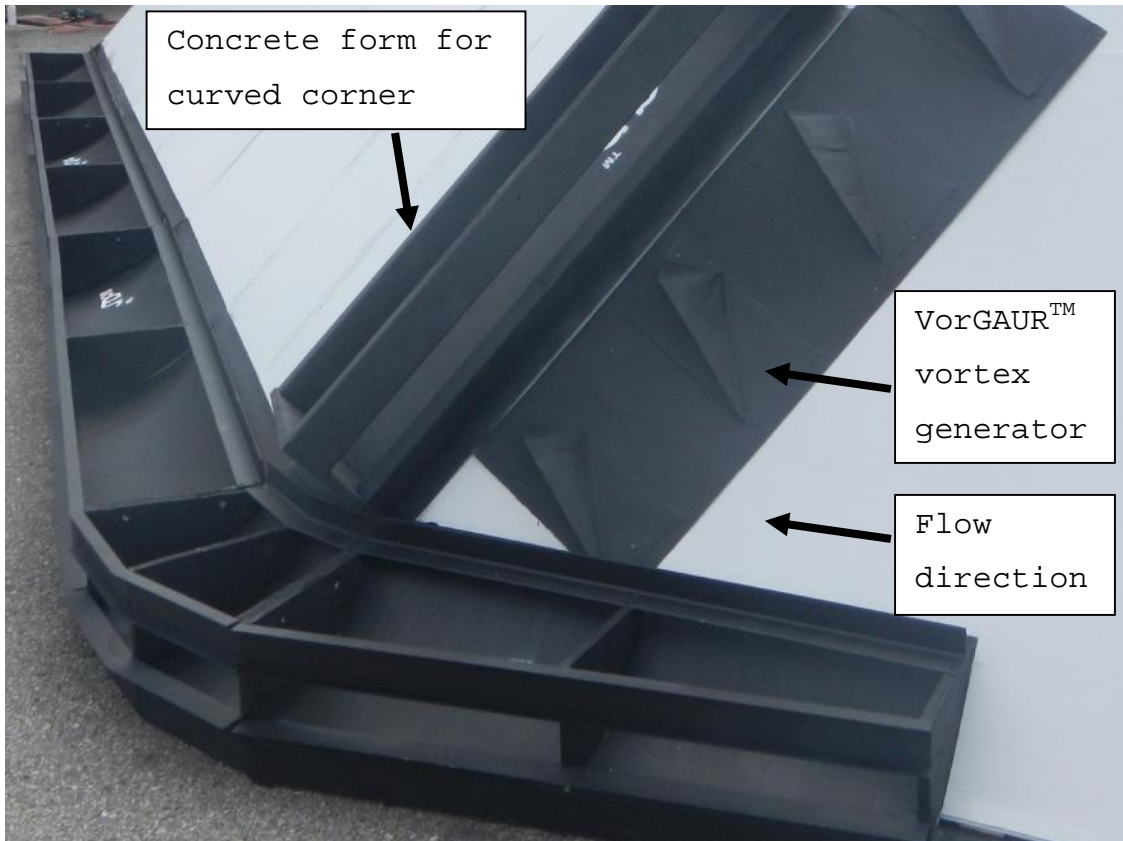


Figure 12. Photo of example sCAUR™ new construction concrete forms (black) for a 45° spill-through abutment. Note stainless steel VorGAUR™ vortex generators mounted after concrete construction.

#### ADDITIONAL EXAMPLE APPLICATIONS

A number of additional applications and detailed drawings are described in US Patent 9,453,319, Sept. 27, 2016. Brief descriptions of the ideas are given below.

#### Example Of Initially Submerged Pier And Abutment Vortex Generators To Protect A Foundation From Open-Bed Scour

In addition to the curved leading edge ramp mentioned above, a further innovation to protect a foundation from open-bed scour uses a vortex generator at 20 degrees angle of attack in front of each leading edge corner of the ramp, which will create a

vortex that brings available loose open-bed scour materials toward the pier or abutment foundation to protect the pier or abutment, as shown in Figure 13 for a pier. Like for the ramp, when there is no high velocity flow and the curved leading edge ramp (7 on figure) is covered with river bed material, the vortex generators (3B on figure) are also covered with bed material. When the water flow speed approaching the pier or abutment is large enough to cause open-bed scour, the bed material over the curved leading edge ramp and the vortex generators will eventually be removed exposing both the ramp and vortex generators. Both the curved leading edge ramp and the vortex generators create vortices that bring loose open-bed material toward the foundation to further protect it from scour.

Another innovation uses vortex generators (VG) mounted on the sides of the foundation to bring more available loose open-bed scour materials toward the pier or abutment foundation to protect further the pier or abutment. These vortex generators are initially submerged below the surface of the river bed, but are exposed when there is high velocity flow and open-bed scour. Properly oriented, they create vortices that bring open-bed scour material towards the foundation for protection.

Figures 14, 15, and 16 show patent drawings of the piece-wise continuous stainless steel retrofits to a pier, wing-wall abutment, and spill-through abutment. Note the use of vortex generators around the foundation to prevent scour when there is open bed scour.

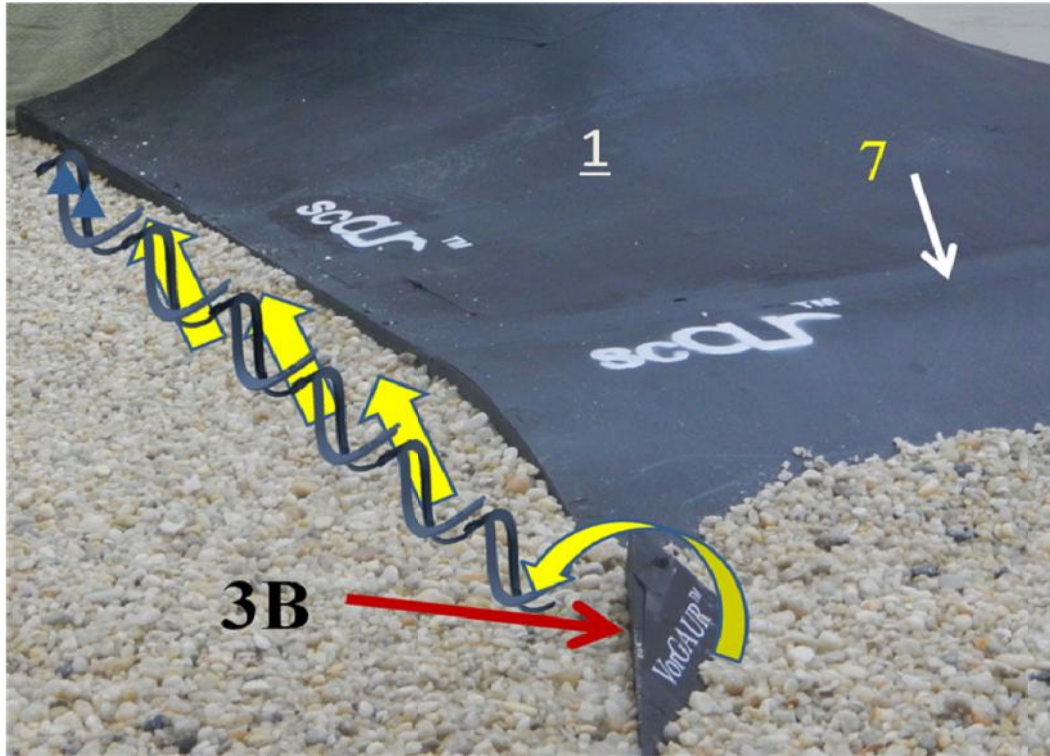


Figure 13 VorGAUR™ vortex generator at left ramp corner creates CCW vortex that brings open-bed scour gravel toward the foundation.

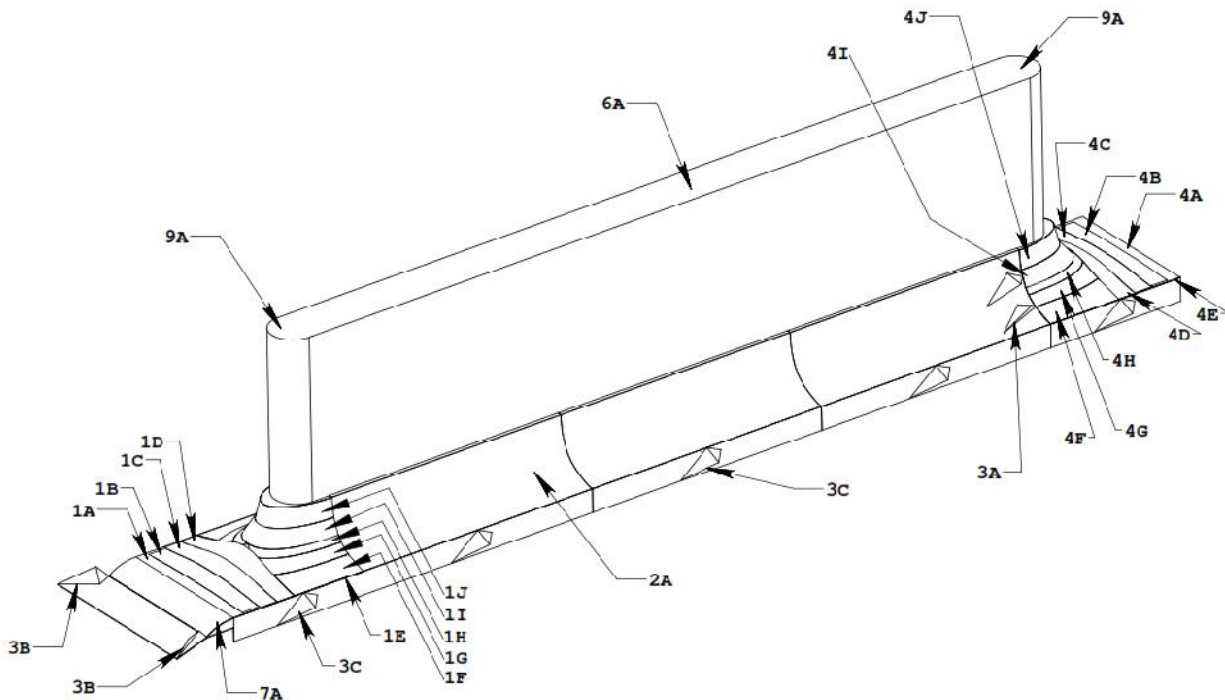


Figure 14. Drawing of a full-scale sheet metal scaUR™ retrofit

fairing with VorGAUR™ for a pier (6A) with piece-wise continuous concave-convex curvature surfaces, with individual sections or pieces of nose surface (1A), (1B), (1C), (1D), (1E), (1F), (1G),(1H),(1I),(1J); for the side of the pier (2A); and the stern or tail, with individual sections or pieces of surface (4A), (4B), (4C), (4D), (4E), (4F),(4G),(4H),(4I), and (4J), within definable tolerances that produce the same effects as continuous concave-convex-curvature surfaces. The leading edge ramp (7A) and pier foundation protecting VGs (3B) mounted on leading edge plate (7B) and (3C) mounted on (1E) and (2A) protect the foundation from open-bed scour.

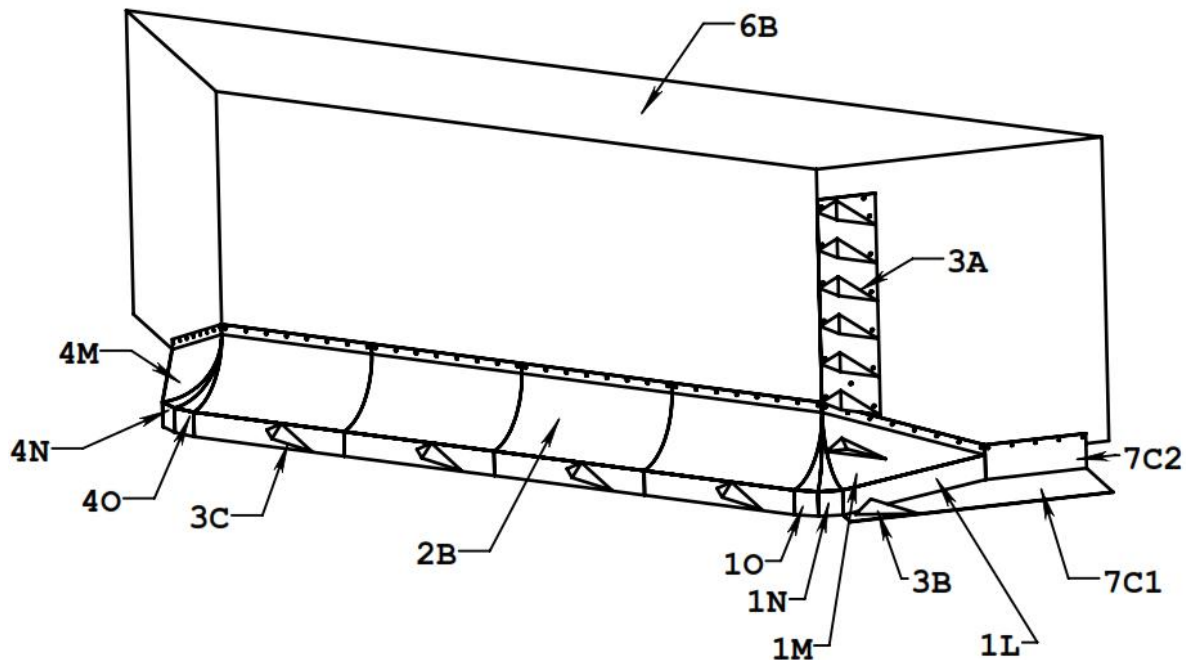


Figure 15. Drawing of full-scale sheet metal scaUR™ retrofit fairing with VorGAUR™ for a wing-wall abutment (6B) with piece-wise continuous concave-convex curvature surfaces consisting of individual sections or pieces of surface (1L), (1M), (1N), (1O), (2B), (4M), (4N), and (4O) within definable tolerances that produce the same effects as continuous concave-convex-curvature surfaces. Vortex generators (3A) reduce the flow separation and free-surface vortex effects while VG (3B) on leading edge

horizontal plate (7C1) that is connected to vertical plate (7C2) and VG (3C) protect the foundation from open-bed scour.

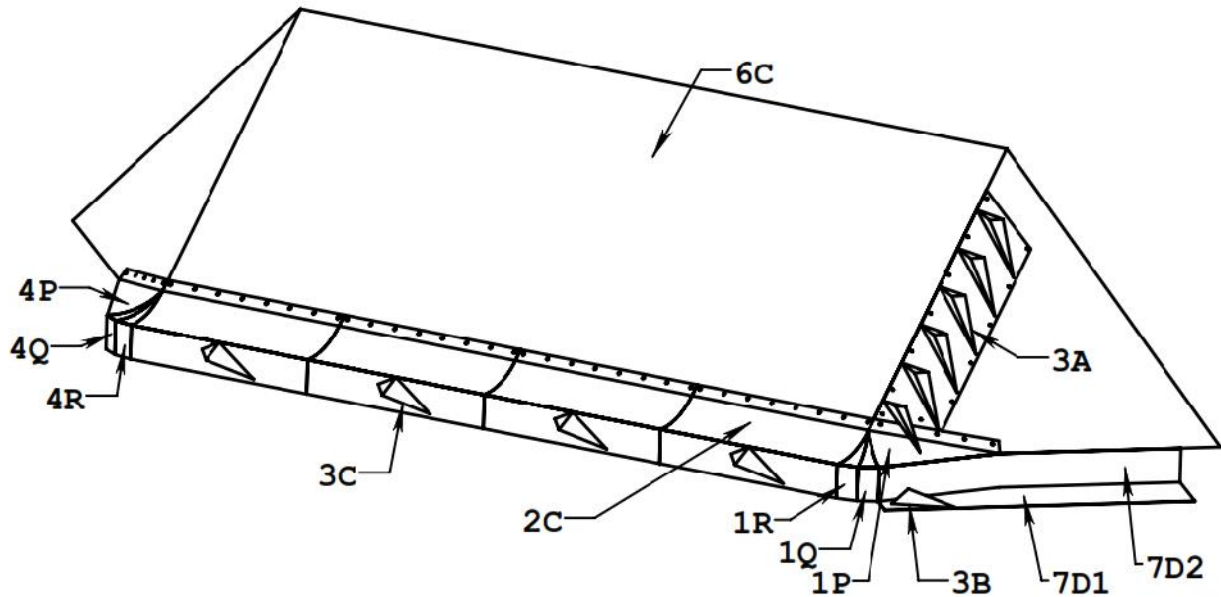


Figure 16. Drawing of full-scale sheet metal sCAUR™ retrofit fairing with VorGAUR™ for a spill-through abutment (6C) with piece-wise continuous concave-convex curvature surfaces consisting of individual sections or pieces of surface (1P), (1Q), (1R), (2C), (4P), (4Q), and (4R) within definable tolerances that produce the same effects as continuous concave-convex-curvature surfaces. Vortex generators (3A) reduce the flow separation and free-surface vortex effects while VG (3B) mounted on leading edge horizontal plate (7D1) connected to vertical plate (7D2) and VG (3C) protect the foundation from open-bed scour.

**Example For Bridge Piers And Abutments At High Angles Of Attack - 45deg Dogleg Configuration**

Here an extension is presented (US Patent 9,453,319) for bridge piers and abutments at larger angles of attack of up to 45°. Nose and tail extension sections on a pier form a dogleg shape (Figure 17) and VorGAUR™ vortex generators prevent separations.

The centerline of the piece-wise continuous curved pier nose and tail extensions and the nose and tail of the scAUR™ are aligned with the on-coming flow direction. VorGAUR™ vortex generators are used to energize the near-wall flow upstream of the adverse pressure gradient regions around the pier and prevent separation and scour. The leading edge ramp and pier foundation protecting VGs mounted on leading edge plate and the sides of the foundation protect the foundation from open-bed scour.

Model scale experiments in the AUR flume were performed that confirm that this design prevents scour. The VGs are attached on both front and rear fairings as shown in Figure 17. The VGs are 76mm long and 19mm high. The free-stream velocity is 0.58m/s and the flow speed near the VGs on the fairings is about 0.61m/s, which caused scour when the VGs were not used. There was no scour around the model.

Manufacturing and installation processes and methods would be the same as for bridges at lower angles of attack that do not need the dogleg. However there are increases in costs due to the addition of the additional components required for the SS dogleg on a pier (8).

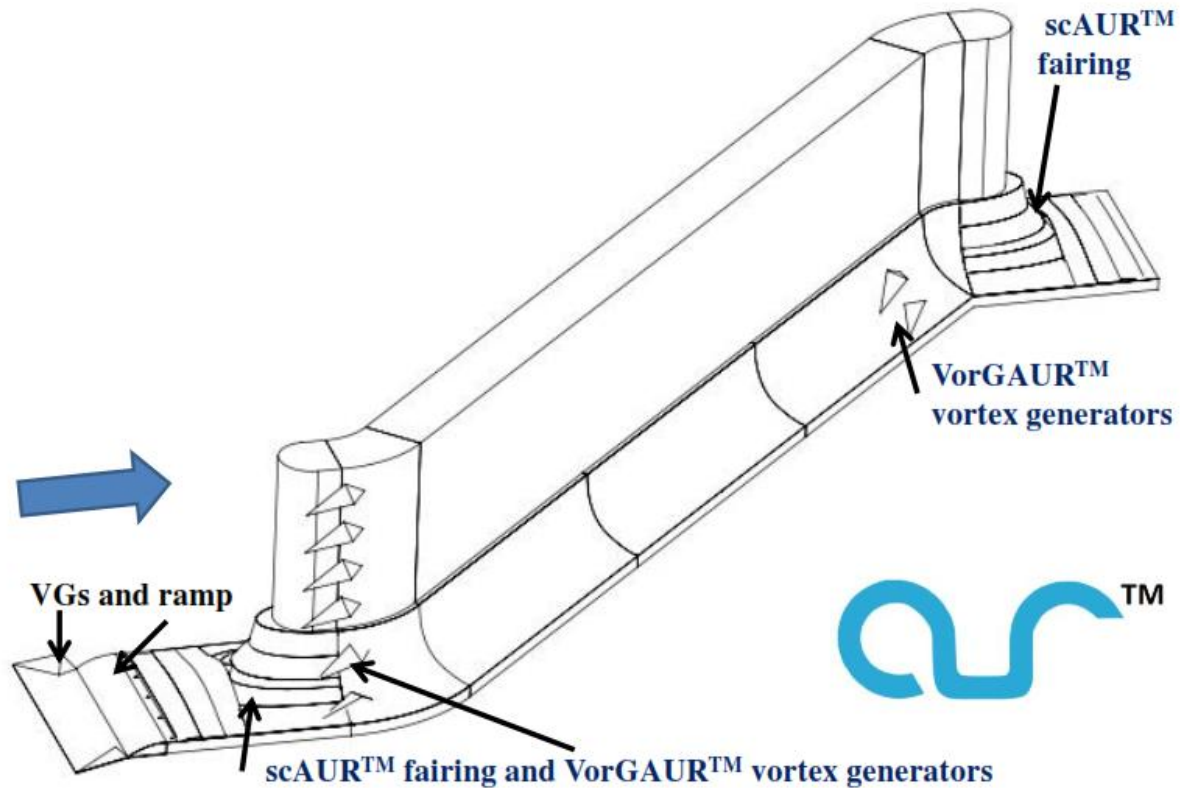


Figure 17. Drawing of a full-scale sheet metal scaUR™ retrofit fairing with VorGAUR™ for a dogleg pier. VGs on the sides of the foundation (not shown here) also protect the pier from open bed scour.

**Example Of Scaur™ With Vorgaur™ For A Swirling River Downstream Of A Bend**

Here another extension is presented (US Patent 9,453,319) for bridge piers and abutments downstream of a bend in a river where there is large-scale swirling approach flow produced by the river bend. The fully three-dimensional shape is modified from the straight ahead case to meet the requirement of the design that the stream-wise gradient of surface vorticity flux must not exceed the vorticity diffusion rate in the boundary layer, thus preventing the formation of a discrete vortex. Another requirement is that a minimal size of the fairing be used that

meets the first requirement.

Figure 18 shows computational fluid dynamics results for a thick upstream inflow boundary layer. The pier is located downstream of a 90 degree river bend. Pier model width  $D$  is 0.076m wide with a 27.5mps flow. The inflow boundary layer thickness = 0.25m. The near-river bottom flow moves toward the inner curved river bank under the large pressure gradient between the inner and outer river banks. The near free-surface flow moves toward the outer curved river bank under the effect of flow inertia. A large stream-wise vortex across the entire river is produced by the end of the curved section of the river.

This swirling flow is the upstream inflow to the pier. This inflow allows one to modify the nose shape from the straight ahead case shape and meet the vorticity flux requirement mentioned above. There is no separation or rollup of a discrete vortex that will cause scour.

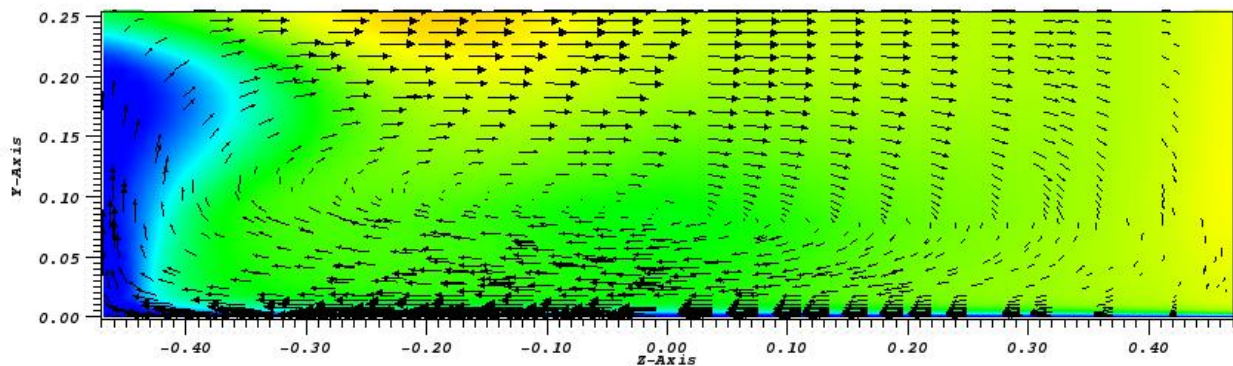


Figure 18. Cross-section of swirling secondary flow from AUR CFD downstream of a 90 degree bend at  $X/D = -0.30$ , but upstream of pier. River surface flow at top of figure moves toward outer river bank on right. Near-wall flow moves toward inner river bank on left.

### Example Pier And Abutment Stern Or Tail Fairings To Further Prevent Scour

When a pier is in close proximity to an adjacent pier or abutment, the flow between the two hydraulic structures is at a higher speed than if they were further apart. This means that at the downstream region of the pier or abutment there will be a greater positive or adverse stream-wise pressure gradient, which will lead to more and stronger flow separation. To reduce this separation and possibilities for scour, a more gradual fairing or tail can be used, as shown in Figure 19 for a pier. A similar more gradual fairing can be used for abutments.

The test with a narrow flume width was conducted without a tail first in order to compare with the tail case. The upstream free-stream flow is 0.56m/s and the flow speed is about 0.66-0.67m/s between the model and the side wall. After 50 minutes the scour holes downstream of the model are symmetric on each side of the centerline and are caused by the separated vortices from the rear fairing. The corresponding scour deposition mound is located along the centerline. A video clip was recorded for this scour development.

A tail is attached to the rear fairing as shown in Figure 19 in order to prevent the separation from the rear fairing which causes this scour hole at the downstream of the model. The tail in this example is a NACA0024 airfoil that is 76mm thick which is the width of model pier, 178mm long and 203mm high.

The tail on the model was tested with the same flume conditions as without a tail, 0.56m/s free-stream velocity and 0.66-0.67m/s between the model and the side wall. After a 50 minutes run with

the same flow speed as before, there are only very minor scour holes generated at the downstream of the model.

## Pier Tail Assembly for Narrow Passages Between Piers and Abutments

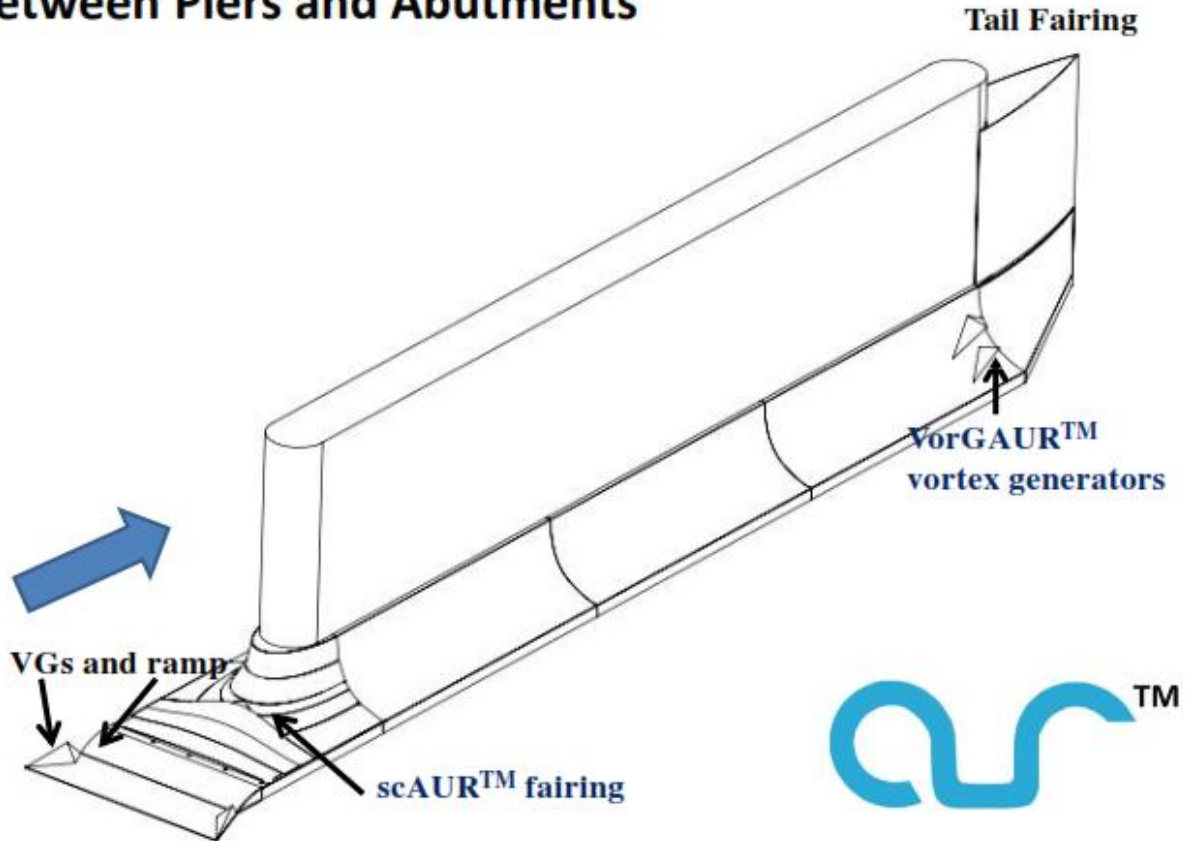


Figure 19. Drawing of full-scale sheet metal retrofit scAUR™ with VorGAUR™ vortex generators for a pier with tail or stern. Vortex generators reduce the flow separation and free-surface vortex effects while VGs (not shown here on foundation) and ramp protect the foundation from open-bed scour.

### CONCLUSIONS

Local scour of bridge piers and abutments is a common cause of highway bridge failures. All currently used countermeasures are temporary and do not prevent the root cause of local scour - discrete large-scaled vortices formed by separations on underwater structures. Using the knowledge of how to prevent the

formation of discrete vortices, prior to the NCHRP-IDEA-162 project, AUR developed, proved using model-scale tests, and patented new local-scouring-vortex-prevention products that are practical cost-effective long-term permanent solutions to the bridge pier and abutment local scour problem. In the NCHRP Project and later work, work on the effect of pier size or scale and model flume tests for other sediments, other abutment designs, and for open bed scour conditions showed that the products prevent scouring vortices and scour. Full-scale prototypes were successfully tested and cost-effective manufacturing and installation plans were developed. **The present value cost of these products over the life of a bridge are an order of magnitude cheaper than current scour countermeasures.** Concrete forms for new bridges and stainless steel retrofit versions for existing bridges are now available. Plans for installation these products on scour-critical bridges are underway.

### **Acknowledgments**

The sCAUR™ and VorGAUR™ were developed first with IR&D funding from AUR, Inc. The new work here was partially supported as Project NCHRP-162 from the NCHRP-IDEA program. The authors appreciate the endorsements and involvement from New Hampshire, Texas, and Virginia DOTs for the NCHRP program.

### **References**

1. Lagasse, P., Zevenbergen, L., Schall, J., and Clopper, P., *Bridge Scour and Stream Instability Countermeasures*. FHWA Technical Report Hydraulic Engineering Circular (HEC)-23, 2001.
2. Flint, M. M., Fringer, O., Billington, S.L., Freyberg, D., and Diffenbaugh, N. S., 2017 *Historical Analysis of Hydraulic Bridge*

*Collapses in the Continental United States*, **ASCE Journal of Infrastructure Systems**, 2017, 23(3), ASCE, ISSN 1076-0342.

3. Briaud, Jean-Louis, *Monitoring Scour Critical Bridges*, NCHRP Synthesis 396, 2006.

4. Ettema, R., Yoon, Byungman, Nakato, Tatsuaki and Muste, Marian, *A review of scour conditions and scour-estimation difficulties for bridge abutments*, **KSCE Journal of Civil Engineering**, Volume 8, Number 6, Pages 643-65, 2004.

5. Sheppard, D.M., Demir, H., and Melville, B., *Scour at Wide Piers and Long Skewed Piers*, NCHRP-Report 682, 2011.

6. Tian, Q.Q., Simpson, R.L., and Lowe, K.T., *A laser-based optical approach for measuring scour depth around hydraulic structures*, **5<sup>th</sup> International Conference on Scour and Erosion**, ASCE, San Francisco, Nov. 7-11, 2010.

7. Barkdoll, B.D., Ettema, R., and B. W. Melville, *Countermeasures to Protect Bridge Abutments from Scour*, NCHRP Report 587, 2007.

8. Simpson, R. L., *Unabridged Report on Full-Scale Prototype Testing and Manufacturing and Installation Plans for New Scour-Vortex-Prevention sCAUR<sup>TM</sup> and VorGAUR<sup>TM</sup> Products for a Representative Scour-critical Bridge*, AUR, Inc., Internal Report NCHRP-162, July 2013.

9. Simpson, R.L. *Turbulent Boundary Layer Separation*, **Annual Review of Fluid Mechanics**, Vol. 21, pp.205-234, 1989.

10. Simpson, R.L., *Aspects of Turbulent Boundary Layer Separation*, **Progress in Aerospace Sciences**, Vol.32, pp.457 - 521, 1996.

11. Simpson, R. L., *Junction Flows*, **Annual Review of Fluid Mechanics**, Vol. 33, pp. 415-443, 2001.

12. Durbin, P.A. and Petterson Reif, B.A., **Statistical Theory and Modeling for Turbulent Flows**, Wiley, 2001.

13. Simpson, R.L., "Some Observations on the Structure and Modeling of 3-D Turbulent Boundary Layers and Separated Flow," **Invited Plenary Lecture, Turbulent Shear Flow Phenomena-4**, Williamsburg, Va, June 27-29, 2005.
14. Sheppard, D.M., Odeh, M., Glasser, T., "Large Scale Clear-Water Local Pier Scour Experiments," **J. Hydraulic Eng.**, ASCE, Vol. 130, pp. 957 -063, 2004.
15. Melville, B., "The Physics of Local Scour at Bridge Piers," **4<sup>th</sup> International Conference on Scour and Erosion**, Tokyo, Japan, 2008.